Available online at www.jbr-pub.org

Open Access at PubMed Central

JBR

The Journal of Biomedical Research, 2014, 28(6):435-446

Invited Review

PET probes beyond ^{18}F-FDG

Lei Jiang[a,b], Yingfeng Tu[b], Hongcheng Shi[a], Zhen Cheng[b,✉]

[a]*Department of Nuclear Medicine, Zhongshan Hospital, Fudan University, 180 Fenglin Road, Shanghai 200032, China;*
[b]*Molecular Imaging Program at Stanford (MIPS), Department of Radiology, Stanford Cancer Institute, Bio-X Program, Canary Center at Stanford for Cancer Early Detection, Stanford University, Stanford, CA 94305, USA.*

Received 10 December 2013, Revised 21 February 2014, Accepted 14 March 2014, Epub 15 April 2014

Abstract

During the past several decades, positron emission tomography (PET) has been one of the rapidly growing areas of medical imaging; particularly, its applications in routine oncological practice have been widely recognized. At present, ^{18}F-fluorodeoxyglucose (^{18}F-FDG) is the most broadly used PET probe. However, ^{18}F-FDG also suffers many limitations. Thus, scientists and clinicians are greatly interested in exploring and developing new PET imaging probes with high affinity and specificity. In this review, we briefly summarize the representative PET probes beyond ^{18}F-FDG that are available for patients imaging in three major clinical areas (oncology, neurology and cardiology), and we also discuss the feasibility and trends in developing new PET probes for personalized medicine.

Keywords: PET, molecular probes, personalized medicine

INTRODUCTION

During the past several decades, positron emission tomography (PET) has been a rapidly growing area of medical imaging, which is increasingly important in routine oncological practice worldwide[1,2]. This change is based on two primary factors: one is the combination of PET and computed tomography (CT), which take advantage of the traditional diagnostic imaging and functional imaging techniques, and the other is the broad utility of ^{18}F-fluorodeoxyglucose (^{18}F-FDG) for evaluating the staging and restaging of cancer, the response to treatment, the differentiation of post-therapy alterations from residual or recurrent tumor, and the assessment of prognoses[3–5].

In 1978, Ido et al.[6] firstly prepared the ^{18}F-FDG using ^{18}F-F2 gas in the Brookhaven National Laboratory of the United States. Another breakthrough was then achieved in 1986 by Hamacher et al.[7], who produced ^{18}F-FDG in high amounts based on ^{18}F-fluoride, and this method was further improved by Fuchtner et al.[8] in 1996. Currently, ^{18}F-FDG, as a biomarker of glucose metabolism, is the most widely used PET probe in clinics (~90%)[1]. After ^{18}F-FDG is injected into the human body, it is taken up by various tissues through glucose transporters and trapped intracellularly. The elevated glycolysis of the cancer cells and a corresponding increase in hexokinase activity lead to the high accumulation of ^{18}F-FDG by cancer cells, which is significantly distinguished from benign tissues. Meanwhile, the accumulation of ^{18}F-FDG is semi-quantified by PET based on the standardized uptake value (SUV; SUV = uptake / [injected dose / patient weight]), which is applied for predicting the likelihood of malignancy[9].

However, ^{18}F-FDG is not a highly specific radiotracer and cannot differentiate between cells that have a high metabolic rate associated with neoplasia and cells with an increased metabolism related to other etiologies, such

✉ Corresponding author: Zhen Cheng, Ph.D., Molecular Imaging Program at Stanford Canary Center at Stanford for Cancer Early Detection, Department of Radiology and Bio-X Program, 1201 Welch Road, Lucas Expansion, P095, Stanford University, Stanford, CA 94305, USA. Tel/Fax: 650-723-7866 (V)/650-736-7925, E-mail: zcheng@stanford.edu.
The authors reported no conflict of interests.

doi: 10.7555/JBR.28.20130196

as infection or inflammation[9]. In addition, many malignancies (such as renal carcinoma) do not display a high accumulation of glucose and are not readily diagnosed by ^{18}F-FDG PET[10–12]. Therefore, scientists and clinicians are greatly interested in exploring and developing other new PET probes, which are able to target some specific biomarkers, are easily transferred from preclinical to clinical settings, and may benefit as many patients as possible.

Many positron-emitting radionuclides may be applied in the development of successful PET radiotracers for research and clinical trials. These radionuclides include, but are not limited to, ^{11}C (Emax 970 keV, half-life [$t_{1/2}$] 20.4 minutes), ^{13}N (Emax 1.30 MeV, $t_{1/2}$ 9.97 minutes), ^{15}O (Emax 1.73 MeV, $t_{1/2}$ 2.04 minutes), ^{18}F (Emax 635 keV, $t_{1/2}$ 109.8 minutes), ^{64}Cu (Emax 657 keV, $t_{1/2}$ 12.7 hours), ^{68}Ga (Emax 1.90 MeV, $t_{1/2}$ 68.1 minutes), ^{82}Rb (Emax 3.36 MeV, $t_{1/2}$ 1.27 minutes), and ^{124}I (Emax 2.13 MeV; 1.53 MeV; 808 keV, $t_{1/2}$ 4.2 days). ^{11}C is an attractive and important positron-emitting radionuclide for labeling molecules targeted to biomarkers. However, the $t_{1/2}$ of ^{11}C is very short (only 20.4 minutes), and multi-steps syntheses are not generally appropriate for the radiosynthesis of ^{11}C-containing molecules; in most cases, ^{11}C is applicable for labeling molecules in academic research and drug development projects[2]. Compared with short half-lived radionuclides, several nonconventional metallic radionuclides with longer half-lives can be prepared in high yields in small biomedical cyclotrons or generators and easily delivered. For example, the availability of ^{68}Ga and ^{82}Rb generators provides an opportunity to prepare PET radiotracers on site if necessary. However, some metallic radionuclides possess complex decay schemes and usually decay with the emission of low β^+-percentage branching (^{86}Y, 33%; ^{68}Ga, 57%), high β^+-energy (^{86}Y, 1.3 MeV; ^{68}Ga, 4.2 MeV), and co-emission of a substantial amount of γ-radiation, which causes patients increased radiation dose. Due to the ideal chemical and nuclear properties of fluorine-18, there has been an increasing focus on establishing tracers labeled with ^{18}F for clinical utility. The half-life of ^{18}F is 109.8 minutes, which is long enough to allow for time-consuming multi-steps radiosyntheses and for imaging procedures to be extended over several hours. Moreover, ^{18}F has a low β^+-energy of 0.64 MeV, which promises a short positron linear range in tissues, resulting in a particularly high spatial resolution of up to 1 mm in PET images and lower radiation doses to patients[2].

At present, the desired imaging targets include cell metabolism (glucose, amino acid, nucleoside, lipid, etc.), biological events (tumor hypoxia, apoptosis, proliferation, angiogenesis, etc.), or many other molecular biomarkers (growth factor receptors, specific enzymes, etc.)[9,13]. Several excellent reviews have summarized the progress of developing PET probes for these important targets[1–2,14]. In the following content, we review the representative PET probes beyond ^{18}F-FDG that are available for patients in three major clinical areas (oncology, neurology and cardiology), and we also discuss the feasibility and trends in developing future PET probes for personalized imaging.

ONCOLOGICAL IMAGING

Imaging tumor amino acid metabolism

Similar to the mechanism of increased glucose transport and corresponding glucose accumulation by tumor cells, most tumor cells exhibit elevated protein synthesis and a high expression of cell membrane transporters of amino acids[15]. Thus, amino acid metabolism is also an important imaging target. Among the various radiolabeled amino acids, L-[methyl-^{11}C] methionine (^{11}C-Met) has been evaluated for a long time. In 1985, Kubota et al.[16] first reported the application of ^{11}C-Met for diagnosing lung tumors. In 1998, Sasaki M et al.[17] demonstrated that ^{11}C-Met PET is useful for distinguishing malignant from benign astrocytomas. More recently, Koizumi et al.[18] reported the usefulness of ^{11}C-Met PET for predicting the response to carbon ion radiotherapy (CIRT) for recurrent rectal cancer. ***Fig. 1*** demonstrates that a patient with the glioblastoma could be diagnosed by ^{11}C-Met PET[19].

Imaging tumor proliferation

As high proliferation is one of the most important characteristics of tumor cells, targeting tumor proliferation (that is, the nucleoside metabolism of tumor cells) is another important imaging goal for exploring new PET probes. Among the radiolabeled nucleoside analogs, ^{11}C-thymidine, a pyrimidine analog that is rapidly incorporated into the DNA of proliferating cells, was initially used[20]. However, the short $t_{1/2}$ of ^{11}C and the rapid degradation of the radiotracer in vivo limited its clinical application[1]. As an alternative to ^{11}C-thymidine, an ^{18}F-labeled pyrimidine analog, ^{18}F-deoxy-3′-fluorothymidine (^{18}F-FLT), was developed and has become widely evaluated in some studies[21–23]. The application of ^{18}F-FLT PET for evaluating proliferation activities has been reported in the diagnosis and evaluation of treatment responses in various types of malignancies, such as lung cancer, brain tumors, breast cancer and lymphoma[24–29]. ***Fig. 2*** presents a case with rectal cancer, which is delineated by both ^{18}F-FLT and ^{18}F-FDG PET[30]. However, negative ^{18}F-FDG uptake

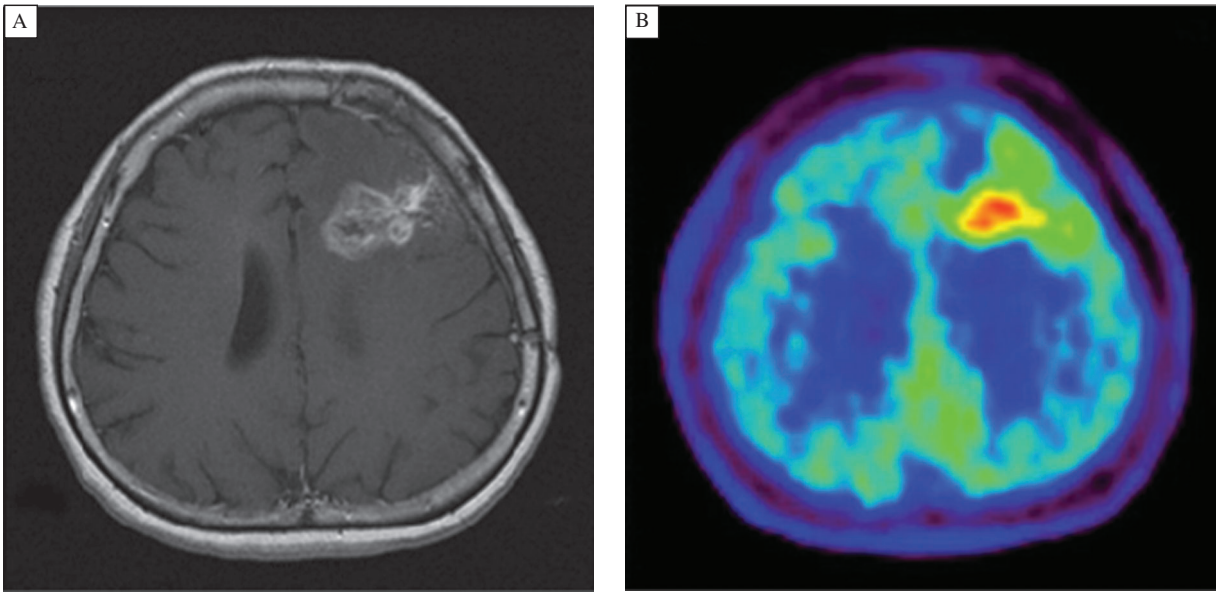

Fig. 1 **Imaging of 49-year-old woman who had been previously treated for glioblastoma multiforme with tumor resection and conventional radiotherapy at dose of 60 Gy (with permission from reference 18).** A: T1-weighted MR image with contrast medium, obtained 13 mo after initial surgery, showing contrast-enhanced lesion in left frontal lobe. B: ^{11}C-Met PET image showing obvious accumulation of tracer corresponding to abnormality on MR image. L/Nmean was 1.70. Recurrent tumor was pathologically confirmed by second surgery.

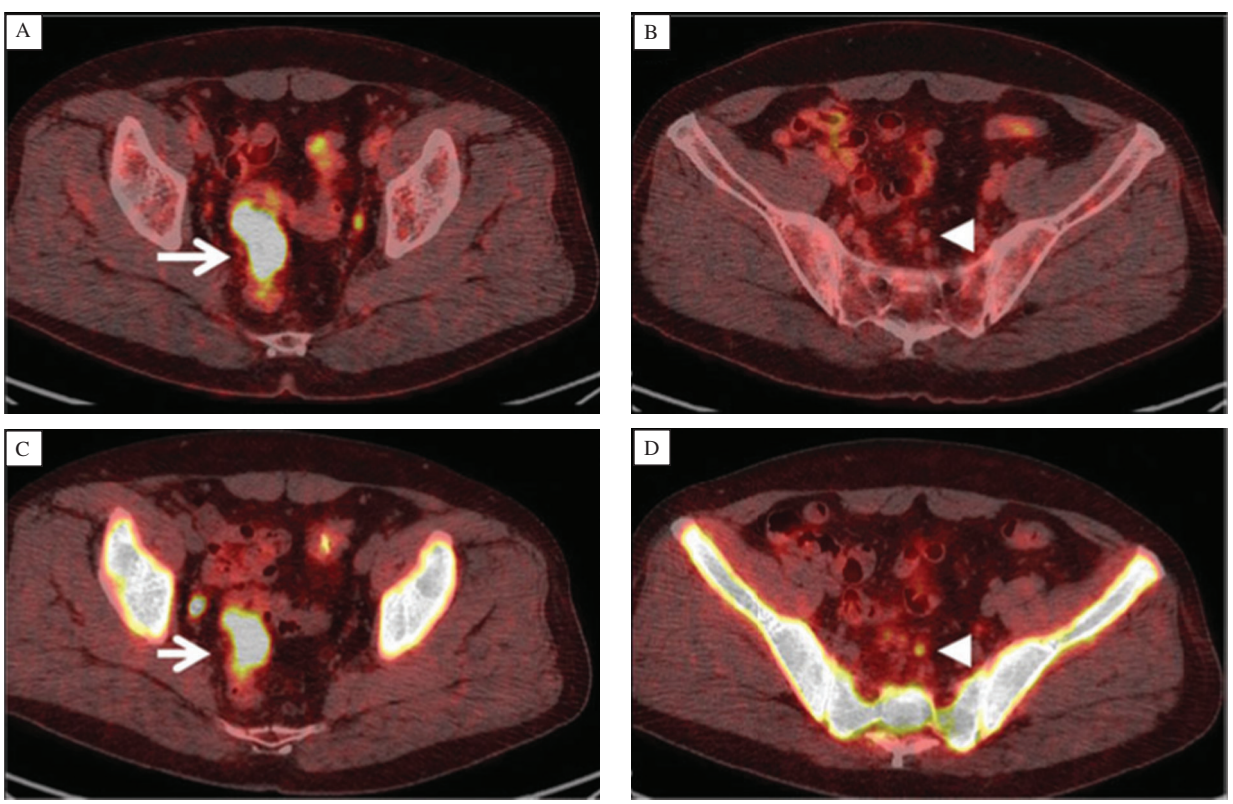

Fig. 2 **A case of rectal cancer with regional metastatic lymph nodes in a 58-year-old man (with permission from reference 29).** A and B: ^{18}F-FDG PET/CT imaging displays positive ^{18}F-FDG uptake in the rectal cancer (SUVmax 25.1, arrow), and negative ^{18}F-FDG uptake in a metastatic regional lymph node (arrowhead). C and D: ^{18}F-FLT PET/CT images show positive ^{18}F-FLT uptake in the rectal cancer (SUV max 7.7, arrow) and in the metastatic regional lymph node (arrowhead).

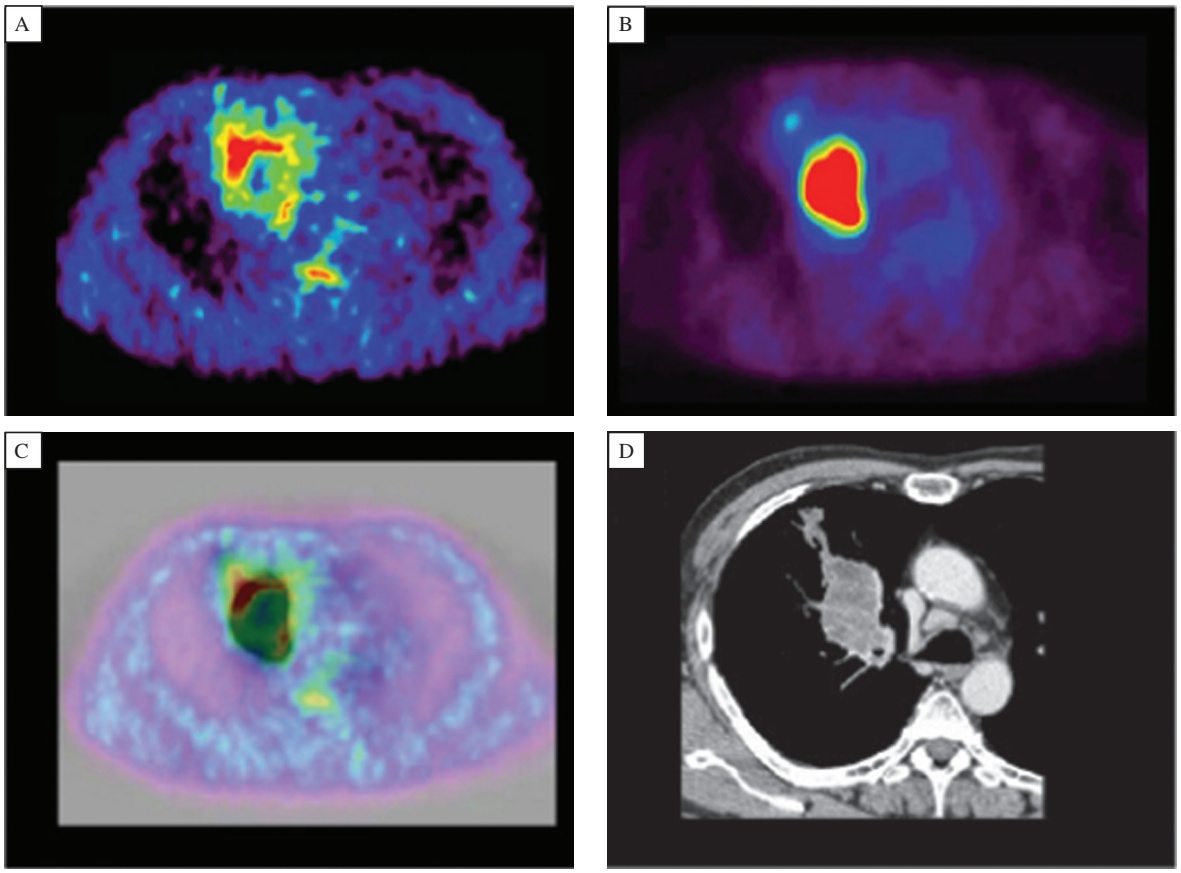

Fig. 3 **^{62}Cu-ATSM (A) and ^{18}F-FDG PET (B) PET images in a patient with squamous cell carcinoma (SCC) (with permission from reference 39).** ^{18}F-FDG image shows intense uptake in the right lung. ^{62}Cu-ATSM image at the corresponding slice level displays high uptake in a region different from the ^{18}F-FDG image. Fusion image (C) is depicted for ^{62}Cu-ATSM PET in color and for ^{18}F-FDG PET in gray scale. CT image (D) at the same level demonstrates soft-tissue density with irregular borders of 53 × 36 mm adjacent to the right mediastinum.

was observed in a metastatic regional lymph node on PET/CT images, but positive ^{18}F-FLT accumulation was seen in the lymph node.

Imaging tumor hypoxia

Tumor hypoxia results from an inadequate supply of oxygen from the vasculature to the growing tumors. Furthermore, the presence of tumor hypoxia promotes a more aggressive phenotype with resistance to treatment, which constitutes a major challenge to patient management, especially in cancer radiotherapy. Therefore, accurate judgment of tumor hypoxia is critical for oncologists to design treatment protocols and to predict treatment outcomes. For this purpose, various PET probes targeting tumor hypoxia have been developed.

At present, there are several PET probes showing high promise for imaging hypoxia. One is an ^{18}F-labeled 2-nitroimidazole derivative, that is, ^{18}F-fluoromisonidazole (^{18}F-FMISO). It has been used to predict the radiotherapy response of tumors (such as lung cancer and head-and-neck cancer) and indicates the prognostic value for patients prior to therapy in investigations[31–34]. However, with the slow blood clearance of ^{18}F-FMISO, the contrast between hypoxic tumors and normal tissues is relatively low, which limits its evaluation of changes in hypoxia during the therapeutic interventions. Another probe is ^{18}F-fluoroazomycin arabinoside (^{18}F-FAZA), a novel 2-nitroimidazole derivative, which has more favorable kinetics than ^{18}F-FMISO does and has displayed promise in imaging tumor hypoxia[35–36]. Moreover, ^{18}F-EF5 is also a validated marker for PET imaging of tumor hypoxia[37].

2-nitroimidazole derivatives, including a novel hypoxic tracer called Cu-diacetyl-bis (N4-methyl-thiosemicarbazone) (Cu-ATSM), which is retained in hypoxic cells, were developed by Fujibayashi et al.[38]. As Cu-ATSM has high membrane permeability and low redox potential, it rapidly enters into cells but is trapped only in hypoxic cells with a reducing environment by the reduction of Cu(II) to Cu(I)[39]. ^{62}Cu-ATSM-PET is currently ongoing in several institutions for studies. ***Fig. 3*** shows the

comparison between ^{62}Cu-ATSM and ^{18}F-FDG PET in a patient with squamous cell carcinoma (SCC)[40].

Imaging tumor apoptosis

Many effective treatments, such as radiation therapy and chemotherapy, may induce an early increase in cell death, often by apoptosis (programmed cell death). Therefore, in vivo apoptosis imaging offers another approach targeting tumor cells to monitor and evaluate anticancer therapy. The most investigation of these radiotracers is Annexin V and its derivatives. In 1999, Blankenberg FG et al.[41] labeled annexin V with ^{99m}Tc for single photon emission computed tomography (SPECT) imaging. However, apoptosis is a relatively rapid progress, and only a fraction of tumor cells are expected to be in the apoptotic state[42]. The annexin V signal is frequently low and not easily detectable by SPECT. Many researches on the evaluation of annexin V radiolabeled with a wide variety of positron-emitting radionuclides (including ^{18}F and ^{11}C) have also been under investigation[43–44]. However, until now, few cases and clinical trials have been reported.

Imaging tumor angiogenesis

Angiogenesis, the formation of new blood vessels from pre-existing vasculature, plays a vital role in tumor growth and metastatic spread. Tumor growth beyond a few millimeters in diameter requires independent vasculatures for the cellular supply of oxygen and nutrients and the removal of waste products. Tumor angiogenesis is a complex, multi-steps process that follows a characteristic sequence of events mediated and controlled by growth factors, cellular receptors and adhesion molecules.

During this process, cell adhesion receptors of the integrin family are responsible for a wide range of cell-extracellular matrix and cell-cell interactions and have been mostly well-studied in many tumors, including glioblastoma, melanoma, ovarian cancer, breast cancer and prostate cancer types[45–46]. One of the most prominent members of this receptor class is $\alpha v\beta 3$ integrin, which is highly expressed on activated endothelial cells. The induced expression of these integrins is crucial for mediating tumor angiogenesis, growth and metastasis. Moreover, $\alpha v\beta 3$ integrin receptors are either not expressed or in very low level on mature vessels or non-neoplastic epithelium.

Many integrins, including $\alpha v\beta 3$ and $\alpha v\beta 5$, are recognized by their extracellular ligands such as the tripeptide Arg-Gly-Asp (RGD) peptides. A large number of $\alpha v\beta 3$ antagonists, including peptidomimetics, knottin and cyclic RGD peptides, radiolabeled with ^{18}F, ^{64}Cu and ^{68}Ga [47–50], have been developed for PET imaging of tumor angiogenesis. Some of them, such as ^{18}F-FPP-RGD_2[51] and ^{18}F-AIF-NOTA-$PRGD_2$ (denoted as ^{18}F-alfatide)[52–53], are currently evolving into clinical trials. As shown in ***Fig. 4***, a case with a primary squamous carcinoma and lymph node metastasis was displayed on ^{18}F-FDG imaging. Meanwhile, ^{18}F-AIF-NOTA-$PRGD_2$ imaging also detected the primary tumor and lymph node metastasis.

Imaging tumor receptors

Receptors for regulatory peptides are overexpressed in various cancer cells and are regarded as important targets for cancer molecular imaging. Many radiolabeled compounds have been developed for the imaging of tumor receptors, and some are under assessment. Receptor imaging can noninvasively evaluate the status of receptor expression in cancerous tissues, which is useful for characterizing the individual cancers, early diagnosis and selecting candidates for receptor-targeted treatment.

For neuroendocrine tumors (NET), somatostatin (SS) receptors are overexpressed on cell surface and are imaged by radiolabeled SS analogs. There are five subtypes of SS receptors, and among these, SS receptor 2 is predominantly expressed in most NETs. In addition to ^{111}In-DTPA-octreotide (^{111}In-DTPAOC) for SPECT imaging, ^{68}Ga-DOTATOC has been proven to have a high affinity with SS receptor 2, which is widely evaluated in the practice of PET imaging (***Fig. 5***)[54–56].

The growth factor receptors are another category of tumor receptors targeted by PET imaging probes. The most extensively studied growth factor receptors suitable for imaging and therapy are the epidermal growth factor receptor (EGFR) and human epidermal growth factor receptor 2 (HER2)[57]. EGFR is a membrane protein comprising an intracellular domain with tyrosine kinase activity, a hydrophobic transmembrane domain and an extracellular ligand-binding domain. Aberrant expression and activation of EGFR is commonly found in human tumors of epithelial origin, where this receptor promotes tumor growth and progression. Several types of PET probes have been used to target EGFR, specifically, monoclonal antibodies, epidermal growth factor, EGFR binding proteins and peptides and EGFR tyrosine kinase inhibitors[58]. The biodistribution and tumor localization of these probes have been evaluated by small animal PET in animal tumor models, and the gefitinib analog ^{11}C-PD153035 has been evaluated in humans by Liu et al.[59] and Fredriksson et al.[60].

The growth factor receptor HER2 is a transmembrane glycoprotein encoded by the HER2/neu proto-oncogene. The amplification and activation of HER2

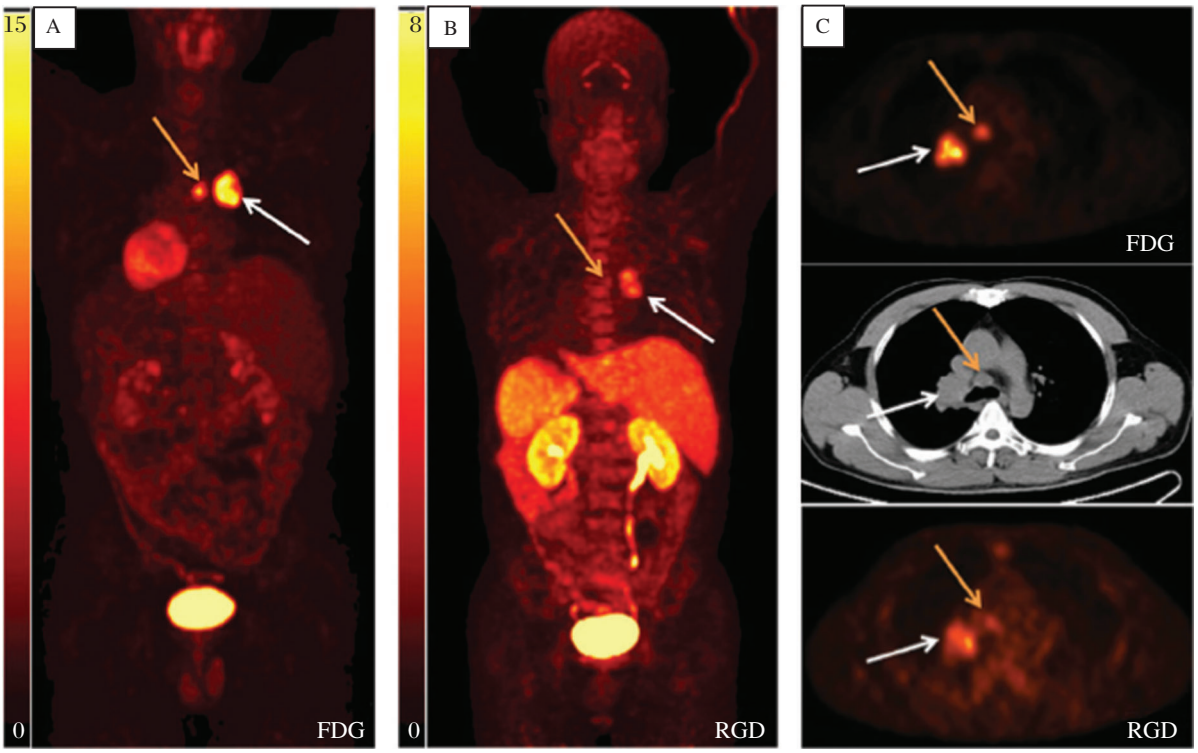

Fig. 4 **^{18}F-FDG (A) and ^{18}F-AIF-NOTA-PRGD$_2$ (B) maximum-intensity-projection imaging of a case with a primary squamous carcinoma (white arrow) and lymph node metastasis (yellow arrow).** C: Transaxial PET image with administration of ^{18}F-FDG (upper) and ^{18}F-AIF-NOTA-PRGD$_2$ (lower) and the corresponding CT image (middle) displaying carcinoma and lymph node metastasis (with permission from reference 52).

promote tumor cell proliferation, growth, migration, adhesion and invasiveness[61]. The *HER2* gene is overexpressed and/or amplified in 20–30% of all primary invasive breast cancers, and high levels of the receptor are closely associated with a poor prognosis of breast cancer[62–63]. At present, many targeting-HER2 chemotherapy drugs have been explored in pre-clinical research and trastuzumab has been widely used in clinic. HER2-PET, as a molecular imaging tool, thus can play important roles in screening patients for HER2 targeted therapy and monitoring treatment efficacy. Currently, the PET probes that target HER2 essentially include monoclonal antibodies (in various engineered formats) and affibodies, which are currently in preclinical evaluation[57].

NEUROLOGICAL IMAGING

Aβ imaging

Alzheimer's disease (AD) is defined histologically by the presence of extracellular β-amyloid (Aβ) plaques and intraneuronal neurofibrillary tangles (NFTs) in the cerebral cortex. The senile or neuritic plaque or Aβ is one of the signature lesions of the AD brain. In 2003, Mathis et al.[64] and Klunk et al.[65] from the University of Pittsburgh Medical Center reported the development of a ^{11}C-labeled PET tracer, 6-OH-BTA ([*N*methyl-] 2-(4=-methylaminophenyl)-6-hydroxybenzothiazole), also known as Pittsburgh compound B or PIB. ^{11}C-PIB both displays a high affinity for aggregated Aβ and provides the high level of brain entry necessary for PET imaging. Based on the PIB molecule, the ^{18}F-labeled analog 3′-^{18}F-PIB was also developed by the Pittsburgh group and is now under evaluation. Moreover, in 2004, Kung et al.[66] from the University of Pennsylvania at Philadelphia developed a small, neutral stilbene derivative, ^{11}C-SB-13, which also demonstrates an excellent binding affinity for Aβ. Additionally, two structurally similar fluoropegylated agents being developed commercially are ^{18}F-AV-45 (shown in ***Fig. 6***) and ^{18}F-AV-1 [1]. Taking ^{18}F-AV-1 as an example, it has been demonstrated to have the potential to distinguish AD from frontotemporal lobe dementia (FTLD). Rowe et al. reported that in a preliminary clinical study, ^{18}F-AV-1 PET imaging displayed extensive cortical accumulation in AD patients but negative in those patients with FTLD. There was no ^{18}F-AV-1 uptake shown in pure vascular dementia or Parkinson's disease (PD), but intermediate grade accumulation of ^{18}F-AV-1 in mild cognitive impairment and dementia with Lewy bodies (DLB)[67].

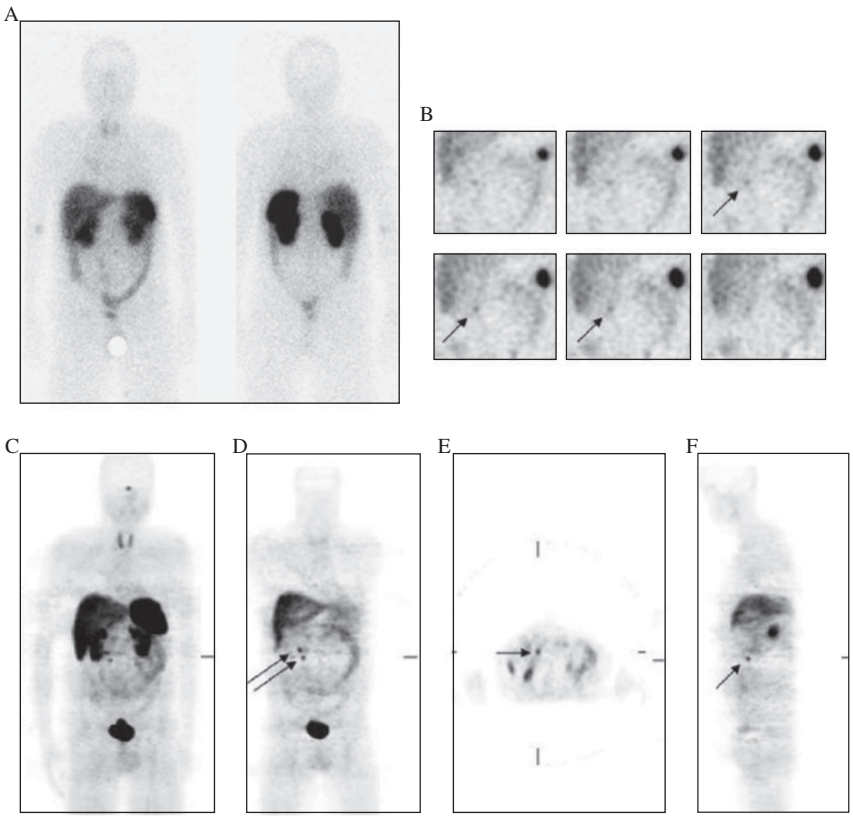

Fig. 5 **SSTR-positive abdominal lymph nodes on the right-hand side (with permission from reference 53).** A and B: ^{111}In-DTPAOC SPECT. a: Planar whole-body scan, 4 hours postinjection. Anterior view (left scan) and posterior view (right scan). There is no certain evidence of pathologically increased uptake in the abdominal lymph nodes. B: ^{111}In-DTPAOC SPECT, 4 hours postinjection. Coronal slices; anterior view. Unifocal, weak uptake is present in a lymph node (arrow) of the right abdomen. C-F: ^{68}Ga-DOTATOC PET. There is evidence of bifocal, intense uptake in two abdominal lymph nodes (arrows). C: maximum intensity projection. D: coronal slice. E: transaxial slice. F: sagittal slice.

Imaging vesicular monoamine transporter type II

In the brain, vesicular monoamine transporter type II (VMAT2) is responsible for the vesicular packaging and storage of monoamine neurotransmitters. In contrast to the situation on the presynaptic membrane, where there are specific and distinct transporters for active reuptake of three monoamines (dopamine, serotonin and norepinephrine), a common adenosine triphosphate-dependent transporter, VMAT2, is responsible for the movement of all three monoamines from the cytosol in the presynaptic neuron into the vesicular lumen. Therefore, imaging VMAT2 in the brain can provide a measurement of the integrity (total number) of all three types of monoaminergic neurons.

During the past decade, a plethora of dopamine transporter imaging probes have been developed, most of which are tropane (or cocaine) derivatives that have varying degrees of affinity to serotonin and norepinephrine transporters. Imaging of the VMAT2 has been proposed as an alternative for monitoring the degeneration of monoaminergic (primarily dopaminergic) neurons in PD. In the 1990s, ^{11}C-(+)-dihydrotetrabenzamine (^{11}C-DTBZ), a radioligand specific for VMA2, was first developed[68–69]. Subsequently, an ^{18}F-labeled fluoropropyl derivative, ^{18}F-FP(+)DTBZ (known as AV-133, from AVID Pharmaceuticals) demonstrated comparable and even better VMAT2 targeting properties than that of ^{11}C-(+)-DTBZ[70].

CARDIAC IMAGING

The application of PET in ischemic heart disease falls within two main categories. First, PET is a well-established imaging modality for the evaluation of myocardial blood flow (MBF). Second, PET has been used to assess myocardial metabolism and viability in patients with ischemic left ventricular (LV) dysfunction. The combined study of MBF or myocardial perfusion imaging (MPI) and metabolism by PET has led to a better understanding of the pathophysiology of ischemic heart disease.

On the one hand, several PET radiopharmaceuticals are available for evaluating the relative distribution of

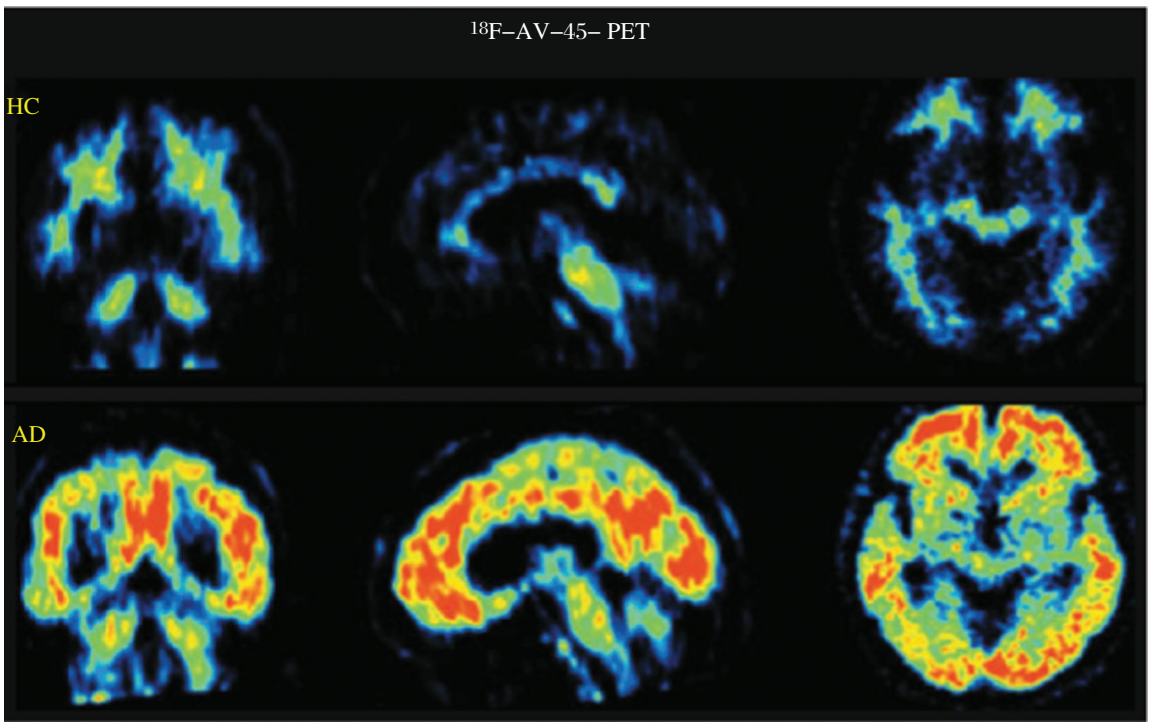

Fig. 6 **^{18}F-AV-45 PET scans in HC (healthy controls) and patients with AD (Alzheimer's disease) (From left to right: coronal, sagittal and transaxial slices).** The accumulation of ^{18}F-AV-45 is correlated with the presence and density of **A**β, and ^{18}F-AV-45 PET scans is a molecular imaging technique that could identify **A**β pathology in the human brain during the lifetime (with permission from reference 1).

MBF, including ^{82}Rb, ^{15}O-water, ^{13}N-ammonia (NH_3) and other agents[71–72]. ^{15}O-water closely meets the requirements for an ideal radiotracer for MBF measurement but with very short half-life. As a K^+ analog, ^{82}Rb is actively transported into myocardial cells via Na^+/K^+ pump. For ^{13}N-NH_3, it is actively transported into myocardial cells via Na^+/K^+ pump or by passive diffusion of neutral lipid soluble ammonia. On the other hand, a PET radiopharmaceutical, ^{18}F-Flurpiridaz, has been explored as a PET probe for MPI studies. ^{18}F-Flurpiridaz, which was also called RP1012[73] or BMS747158[74], is a member of the class of potentiometric lipophilic phosphonium cations originally developed to measure the mitochondrial membrane potential[73–76]. Based on the preclinical research, it has been observed that high and flow-independent first-pass extraction fraction promises linearity between tracer uptake and MBF. The first human results of BMS747158 were presented at the 2010 SNM annual meeting and then published on the Journal of Nuclear Medicine, and the images demonstrate excellent quality (***Fig. 7***)[77].

PERSONALIZED IMAGING MEDICINE

The development of new PET probes begins with target identification and functional analysis, followed by probe development, evaluation in animal models, and finally, the probes are evaluated for their usefulness in clinical settings. To achieve and foster the development of PET probes from preclinical to clinical applications, cooperative efforts are required from biologists to identify and validate novel imaging targets; from chemists and radiochemists to synthesize and optimize PET probes; and from engineers and physicists to develop and explore advanced imaging devices and instruments, such as PET/MRI or PET/optical imaging (OI) and FDA, to accept and approve the clinical trials in human studies.

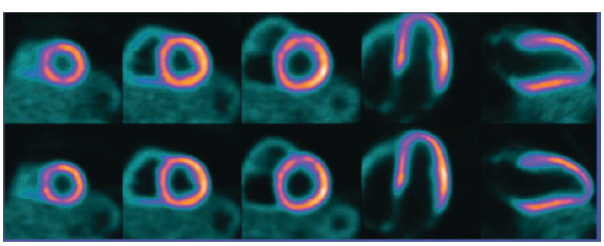

Fig. 7 **Myocardial perfusion imaging based on PET with 18F-BMS747158 (^{18}F-Flurpiridaz).** Upper row, standard reconstruction; Lower row, high-definition cardiac perfusion PET (with permission from reference 75).

As shown in ***Fig. 8***, the time intensive and expensive preclinical steps are involved in drug development[78]. Molecular contrast agent design and clinical use involve

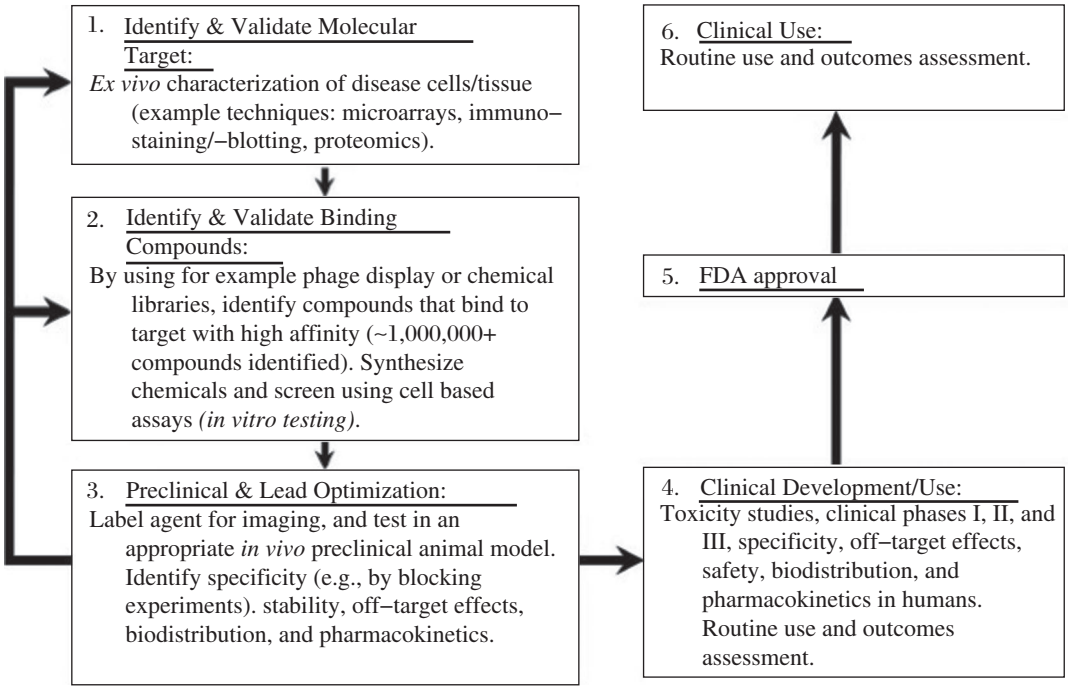

Fig. 8 **The design and clinical use of molecular imaging probes involve a series of steps (with permission from reference 76).** Preclinical steps (green-shaded boxes) involve target identification, validation, chemical labeling, in vitro cellular characterization, and in vivo animal testing. After many optimized steps (arrows between boxes 1, 2 and 3), the imaging probes can be tested in humans after FDA applications for investigatory new drugs (INDs) or exploratory INDs (eINDs). Clinical testing (orange boxes) involves rigorous testing for agent properties (effectiveness, specificity, toxicity, off-target effects, kinetics, etc.) before potential FDA approval for routine clinical practice, which is also heavily monitored for the response to outcomes.

a series of steps similar to those used in drug development, including molecular target identification, validation, chemical synthesis and characterization (in vitro and in vivo testing for activity, specificity, biodistribution, pharmacokinetics, off-target effects, toxicity, etc.) for new molecular imaging probes. In fact, the majority of current molecular imaging agents used in the clinic were initially discovered through these exhaustive preclinical experiments at academic institutions[79]. However, as high investment required for imaging probe development and potential limited profit comparing to therapeutics, developing an FDA approved PET probe for clinical use is highly changeling. The creative solutions for translation and approval the use of the personalized probes should be explored and figured out by researchers and clinicians.

Personalized imaging probes and personalized medicine are necessary and important. First, although it is estimated that a molecular imaging agent costs approximately $150 million over 10 years to discover, test and move to the clinic, the ultimate yield would be a $200–400 million per year revenue for successful contrast agents[79]. Second but more importantly, at present, healthcare spending accounts for almost 18% of the United States gross domestic product (GDP) and is growing rapidly, with projections by the Centers for Medicare & Medicaid Services (CMS) that it will reach 20% of the GDP by 2021 if allowed to grow at the current rate[80–81]. The vast majority of current healthcare dollars goes to treatment, with only a small fraction of total expenditures devoted to prediction, diagnosis and treatment monitoring[81]. The personalized imaging probes are expected to guide the treatment for patients, especially the targeted treatment, and significantly improve healthcare delivery with the potential to reduce costs simultaneously. Finally, molecular imaging and therapy can be integrated, whereby a biologically targeted agent provides both efficient contrast for molecular imaging and the delivery vehicle for molecular therapeutics[81].

CONCLUSION

Currently, PET probes beyond ^{18}F-FDG are widely explored and developed, and several PET probes have been applied in clinical practice or clinical trials. Thus, in the foreseeable future, although ^{18}F-FDG will continue to be used in clinics, an increasing number of target specific PET probes will be widely and routinely used in clinical practice, which will greatly contribute to realize personalized medicine.

References

[1] Vallabhajosula S, Solnes L, Vallabhajosula B. A broad overview of positron emission tomography radiopharmaceuticals and clinical applications: what is new? *Semin Nucl Med* 2011;41:246–64.

[2] Chen K, Chen X. Positron emission tomography imaging of cancer biology: current status and future prospects. *Semin Oncol* 2011;38:70–86.

[3] Gambhir SS, Czernin J, Schwimmer J, Silverman DH, Coleman RE, Phelps ME. A tabulated summary of the FDG PET literature. *J Nucl Med* 2001;42:1S–93S.

[4] Lindsay MJ, Siegel BA, Tunis SR, Hillner BE, Shields AF, Carey BP, et al. The National Oncologic PET Registry: expanded medicare coverage for PET under coverage with evidence development. *AJR Am J Roentgenol* 2007;188: 1109–13.

[5] Beyer T, Townsend DW, Brun T, Kinahan PE, Charron M, Roddy R, et al. A combined PET/CT scanner for clinical oncology. *J Nucl Med* 2000;41:1369–79.

[6] Ido T, Wan CN, Fowler JS. Fluorination with F2: convenient synthesis of 2-deoxy-2-fluoro-d-glucose. *J Org Chem* 1977;42:2341–2.

[7] Hamacher K, Coenen HH, Stöcklin G. Efficient stereospecific synthesis of no-carrier-added 2-[18F]-fluoro-2-deoxy-d-glucose using aminopolyether supported nucleophilic substitution. *J Nucl Med* 1986;27:235–8.

[8] Füchtner F, Steinbach J, Mäding P. Basic previous term hydrolysis next term 2-[18F]fluoro-1,3,4,6-tetra-O-acetyl-image-glucose in the preparation of 2-[18F]fluoro-2-deoxy-Image-glucose. *Appl Radiat Isot* 1996;47:61–6.

[9] Chen K, Conti PS. Target-specific delivery of peptide-based probes for PET imaging. *Adv Drug Deliv Rev* 2010; 62:1005–22.

[10] Kayani I, Groves AM. 18F-fluorodeoxyglucose PET/CT in cancer imaging. *Clin Med* 2006;6:240–4.

[11] Kelloff GJ, Hoffman JM, Johnson B, Scher HI, Siegel BA, Cheng EY, Cheson BD, et al. Progress and promise of FDG-PET imaging for cancer patient management and oncologic drug development. *Clin Cancer Res* 2005; 2785–808.

[12] Rohren EM, Turkington TG, Coleman RE. Clinical applications of PET in Oncology. *Radiology* 2004;231:305–32.

[13] Josephs D, Spicer J, O'Doherty M. Molecular imaging in clinical trials. *Target Oncol* 2009;4:151–68.

[14] Coenen HH, Elsinga PH, Iwata R, Kilbourn MR, Pillai MR, Rajan MG, et al. Fluorine-18 radiopharmaceuticals beyond [18F]FDG for use in oncology and neurosciences. *Nucl Med Biol* 2010;37:727–40.

[15] Jager PL, Vaalburg W, Pruim J, de Vries EG, Langen KJ, Piers DA. Radiolabeled amino acids: Basic aspects and clinical applications in oncology. *J Nucl Med* 2001;42:432–45.

[16] Kubota K, Matsuzawa T, Ito M, Ito K, Fujiwara T, Abe Y, Yoshioka S, et al. Lung tumor imaging by positron emission tomography using C-11 L-methionine. *J Nucl Med* 1985;26:37–42.

[17] Sasaki M, Kuwabara Y, Yoshida T, Nakagawa M, Fukumura T, Mihara F, et al. A comparative study of thallium-201 SPET, carbon-11 methionine PET and fluorine-18 fluorodeoxyglucose PET for the differentiation of astrocytic tumours. *Eur J Nucl Med* 1998;25:1261–9.

[18] Koizumi M, Saga T, Yoshikawa K, Suzuki K, Yamada S, Hasebe M, et al. L-[11C]methyl-methionine positron emission tomography for evaluation of carbon ion radiotherapy in patients with pelvic recurrence of rectal cancer. *Mol Imaging Biol* 2008;10:374–80.

[19] Terakawa Y, Tsuyuguchi N, Iwai Y, Yamanaka K, Higashiyama S, Takami T, et al. Diagnostic accuracy of 11C-methionine PET for differentiation of recurrent brain tumors from radiation necrosis after radiotherapy. *J Nucl Med* 2008;49:694–9.

[20] Christman D, Crawford EJ, Friedkin M, Wolf AP. Detection of DNA synthesis in intact organisms with positron-emitting methyl-[C-11]-thymidine. *Proc Natl Acad Sci U S A* 1972;69:988–92.

[21] Shields AF. PET imaging with 18F-FLT and thymidine analogs: promise and pitfalls. *J Nucl Med* 2003;44:1432–4.

[22] Bading JR, Shields AF. Imaging of cell proliferation: status and prospects. *J Nucl Med* 2008;49:64S–80S.

[23] Salskov A, Tammisetti VS, Grierson J, Vesselle H. FLT: measuring tumor cell proliferation in vivo with positron emission tomography and 3-deoxy-3-[18F]fluorothymidine. *Semin Nucl Med* 2007;37:429–39.

[24] Saga T, Koizumi M, Inubushi M, Yoshikawa K, Tanimoto K, Fukumura T, et al. PET/CT with 3′-deoxy-3′-[18F]fluorothymidine for lung cancer patients receiving carbon-ion radiotherapy. *Nucl Med Commun* 2011;32:348–55.

[25] Been LB, Suurmeijer AJ, Cobben DC, Jager PL, Hoekstra HJ, Elsinga PH. [18F]FLT-PET in oncology: current status and opportunities. *Eur J Nucl Med Mol Imaging* 2004;31:1659–72.

[26] Buck AK, Halter G, Schirrmeister H, Kotzerke J, Wurziger I, Glatting G, et al. Imaging proliferation in lung tumors with PET: 18F-FLT versus 18F-FDG. *J Nucl Med* 2003;44:1426–31.

[27] Chen W, Cloughesy T, Kamdar N, Satyamurthy N, Bergsneider M, Liau L, et al. Imaging proliferation in brain tumors with 18F-FLT PET: comparison with 18F-FDG. *J Nucl Med* 2005;46:945–52.

[28] Saga T, Kawashima H, Araki N, Takahashi JA, Nakashima Y, Higashi T, et al. Evaluation of primary brain tumors with FLT-PET: usefulness and limitations. *Clin Nucl Med* 2006;31:774–80.

[29] Yang YJ, Ryu JS, Kim SY, Oh SJ, Im KC, Lee H, Lee SW, et al. Use of 3′-deoxy-3′-[18F]fluorothymidine PET to monitor early responses to radiation therapy in murine SCCVII tumors. *Eur J Nucl Med Mol Imaging* 2006;33:412–9.

[30] Nakajo M, Nakajo M, Kajiya Y, Jinguji M, Nishimata N, Shimaoka S, et al. Diagnostic performance of ^{18}F-fluorothymidine PET/CT for primary colorectal cancer and its lymph node metastasis: comparison with ^{18}F-fluorodeoxyglucose PET/CT. *Eur J Nucl Med Mol Imaging* 2013;40:1223–32.

[31] Nunn A, Linder K, Strauss HW. Nitroimidazoles and imaging hypoxia. *Eur J Nucl Med* 1995;22:265–80.

[32] Lee ST, Scott AM. Hypoxia positron emission tomography imagimg with 18F-fluoromisonidazole. *Semin Nucl Med* 2007;37:451–61.

[33] Eschmann SM, Paulsen F, Reimold M, Dittmann H, Welz S, Reischl G, et al. Prognostic impact of hypoxia imaging with 18F-misonidazole PET in non-small cell lung cancer and head and neck cancer before radiotherapy. *J Nucl Med* 2005;46:253–60.

[34] Rajendran JG, Schwartz DL, O'Sullivan J, Peterson LM, Ng P, Scharnhorst J, et al. Tumor hypoxia imaging with [F-18]fluoromisonidazole positron emission tomography in head and neck cancer. Clin *Cancer Res* 2006;12:5435–41.

[35] Piert M, Machulla HJ, Picchio M, Reischl G, Ziegler S, Kumar P, et al. Hypoxia-specific tumor imaging with 18F-fluoroazomycin arabinoside. *J Nucl Med* 2005;46: 106–13.

[36] Havelund BM, Holdgaard PC, Rafaelsen SR, Mortensen LS, Theil J, Bender D, et al. Tumour hypoxia imaging with 18F-fluoroazomycinarabinofuranoside PET/CT in patients with locally advanced rectal cancer. *Nucl Med Commun* 2013;34:155–61.

[37] Chitneni SK, Bida GT, Yuan H, Palmer GM, Hay MP, Melcher T, et al. 18F-EF5 PET imaging as an early response biomarker for the hypoxia-activated prodrug SN30000 combined with radiation treatment in a non-small cell lung cancer xenograft model. *J Nucl Med* 2013;54:1339–46.

[38] Fujibayashi Y, Taniuchi H, Yonekura Y, Ohtani H, Konishi J, Yokoyama A. Copper-62-ATSM: a new hypoxia imaging agent with high membrane permeability and low redox potential. *J Nucl Med* 1997;38:1155–60.

[39] Maurer RI, Blower PJ, Dilworth JR, Reynolds CA, Zheng Y, Mullen GE. Studies on the mechanism of hypoxic selectivity in copper bis(thiosemicarbazone) radiopharmaceuticals. *J Med Chem* 2002;45:1420–31.

[40] Lohith TG, Kudo T, Demura Y, Umeda Y, Kiyono Y, Fujibayashi Y, et al. Pathophysiologic correlation between 62Cu-ATSM and 18F-FDG in lung cancer. *J Nucl Med* 2009;50:1948–53.

[41] Blankenberg FG, Katsikis PD, Tait JF, Davis RE, Naumovski L, Ohtsuki K, et al. Imaging of apoptosis (programmed cell death) with 99mTc annexin V. *J Nucl Med* 1999;40:184–91.

[42] Haas RL, de Jong D, Olmos RA, Hoefnagel CA, van den Heuvel I, Zerp SF, et al. In vivo imaging of radiation-induced apoptosis in follicular lymphoma patients. *Int J Radiat Oncol Biol Phys* 2004;59:782–7.

[43] Yagle KJ, Eary JF, Tait JF, Grierson JR, Link JM, Lewellen B, et al. Evaluation of 18F-Annexin V as a PET imaging agent in an animal model of apoptosis. *J Nucl Med* 2005;46:658–66.

[44] Cheng Q, Lu L, Grafström J, Olofsson MH, Thorell JO, Samen E, Johansson K, et al. Combining [11C]-AnxA5 PET imaging with serum biomarkers for improved detection in live mice of modest cell death in human solid tumor xenografts. *PLoS One* 2012;7:e42151.

[45] Hynes RO. Integrins: versatility, modulation, and signaling in cell adhesion. *Cell* 1992;69:11–25.

[46] Seftor RE, Seftor EA, Gehlsen KR, Stetler-Stevenson WG, Brown PD, Ruoslahti E, et al. Role of the αvβ3 integrin in human melanoma cell invasion. *Pro Natl Acad Sci USA* 1992;89:1557–61.

[47] Cheng Z, Wu Y, Xiong Z, Gambhir SS, Chen X. Near-infrared fluorescent RGD peptides for optical imaging of integrin αvβ3 expression in living mice. *Bioconjug Chem* 2005;16:1433–41.

[48] Li ZB, Cai W, Cao Q, Chen K, Wu Z, He L, et al. (64)Cu-labeled tetrameric and octameric RGD peptides for small-animal PET of tumor alpha(v)beta(3) integrin expression. *J Nucl Med* 2007;48:1162–71.

[49] Liu S. Radiolabeled cyclic RGD peptides as integrin alpha(v)beta(3)-targeted radiotracers: maximizing binding affinity via bivalency. *Bioconjug Chem* 2009;20:2199–213.

[50] Jiang L, Kimura RH, Miao Z, Silverman AP, Ren G, Liu H, et al. Evaluation of a (64)Cu-labeled cystine-knot peptide based on agouti-related protein for PET of tumors expressing αvβ3 integrin. *J Nucl Med* 2010;51:251–8.

[51] Chin FT, Shen B, Liu S, Berganos RA, Chang E, Mittra E, et al. First Experience with Clinical-Grade [18F]FPP(RGD)2: An Automated Multi-step Radiosynthesis for Clinical PET Studies. *Mol Imaging Biol* 2012;14:88–95.

[52] Liu S, Liu H, Jiang H, Xu Y, Zhang H, Cheng Z. One-step radiosynthesis of 18F-AlF-NOTA-RGD2 for tumor angiogenesis PET imaging. *Eur J Nucl Med Mol Imaging* 2011;38:1732–41.

[53] Wan W, Guo N, Pan D, Yu C, Weng Y, Luo S, Ding H, et al. First experience of 18F-alfatide in lung cancer patients using a new lyophilized kit for rapid radiofluorination. *J Nucl Med* 2013;54:691–8.

[54] Buchmann I, Henze M, Engelbrecht S, Eisenhut M, Runz A, Schäfer M, et al. Comparison of 68Ga-DOTATOC PET and 111In-DTPAOC (Octreoscan) SPECT in patients with neuroendocrine tumours. *Eur J Nucl Med Mol Imaging* 2007;34:1617–26.

[55] Rufini V, Calcagni ML, Baum RP. Imaging of neuroendocrine tumors. *Semin Nucl Med* 2007;36:228–247.

[56] Gabriel M, Decristoforo C, Kendler D, Dobrozemsky G, Heute D, Uprimny C, et al. 68Ga-DOTA-Tyr3-octreotide PET in neuroendocrine tumors: comparison with somatostatin receptor scintigraphy and CT. *J Nucl Med* 2007:508–18.

[57] Del Vecchio S, Zannetti A, Fonti R, Iommelli F, Pizzuti LM, Lettieri A, et al. PET/CT in cancer research: from preclinical to clinical applications. *Contrast Media Mol Imaging* 2010;5:190–200.

[58] Cai W, Niu G, Chen X. Multimodality imaging of the HER-kinase axis in cancer. *Eur J Nucl Med Mol Imag* 2008;35:186–208.

[59] Liu N, Li M, Li X, Meng X, Yang G, Zhao S, et al. PET-based biodistribution and radiation dosimetry of epidermal growth factor receptor-selective tracer 11C-PD153035 in humans. *J Nucl Med* 2009;50:303–8.

[60] Fredriksson A, Johnstrom P, Thorell JO, von Heijne G, Hassan M, Eksborg S, et al. In vivo evaluation of the biodistribution of 11C-labeled PD153035 in rats without and with neuroblastoma implants. *Life Sci* 1999;65:165–74.

[61] Sergina NV, Moasser MM. The HER family and cancer: emerging molecular mechanisms and therapeutic targets. *Trends Mol Med* 2007;13:527–34.

[62] Di Cosimo S, Baselga J. Targeted therapies in breast cancer: where are we now? *Eur J Cancer* 2008;44:2781–90.

[63] Nielsen DL, Andersson M, Kamby C. HER2-targeted therapy in breast cancer. Monoclonal antibodies and tyrosine kinase inhibitors. *Cancer Treat Rev* 2009;35:121–36.

[64] Mathis CA, Wang Y, Holt DP, Huang GF, Debnath ML, Klunk WE. Synthesis and evaluation of 11Clabeled 6-substituted 2-aryl benzothiazoles as amyloid imaging agents. *J Med Chem* 2003;46:2740–54.

[65] Klunk WE, Engler H, Nordberg A, Wang Y, Blomqvist G, Holt DP, et al. Imaging brain amyloid in Alzheimer's

disease with Pittsburgh compound-B. *Ann Neurol* 2004; 55:306–19.

[66] Kung M-P, Hou C, Zhuang Z-P, Skovronsky D, Kung HF. Binding of two potential imaging agents targeting amyloid plaques in postmortem brain tissues of patients with Alzheimer′s disease. *Brain Res* 2004;1025:98–105.

[67] Rowe CC, Ackerman U, Browne W, Mulligan R, Pike KL, O′Keefe G, et al. Imaging of amyloid beta in Alzheimer′s disease with 18F-BAY94-9172, a novel PET tracer: proof of mechanism. *Lancet Neurol* 2008;7:129–35.

[68] Kilbourn MR. In vivo radiotracers for vesicular neurotransmitter transporters. *Nucl Med Biol* 1997;24:615–9.

[69] Frey KA, Koeppe RA, Kilbourn MR, Vander Borght TM, Albin RL, Gilman S, et al. Presynaptic monoaminergic vesicles in Parkinsons′s disease and normal aging. *Ann Neurol* 1996;40:873–84.

[70] Kung M-P, Hou C, Goswami R, Ponde DE, Kilbourn MR, Kung HF. Characterization of optically resolved 9-fluoropropyl-dihydrotetrabenazine as a potential PET imaging agent targeting vesicular monoamine transporters. *Nucl Med Biol* 2007;34:239–46.

[71] Schelbert HR. Positron emission tomography of the heart: methodology, findings in the normal and disease heart, and clinical applications, in Phelps ME, (ed): PET: Molecular Imaging and Its Clinical Applications. New York, Springer, 2004.

[72] Lin JW, Sciacca RR, Chou RL, Laine AF, Bergmann SR. Quantification of myocardial perfusion in human subjects using 82 Rb and wavelet-based noise reduction. *J Nucl Med* 2001;42:201–8.

[73] Yalamanchili P, Wexler E, Hayes M, Yu M, Bozek J, Kagan M, et al. Mechanism of uptake and retention of F-18 BMS-747158-02 in cardiomyocytes: a novel PET myocardial imaging agent. *J Nucl Cardiol* 2007;14:782–8.

[74] Yu M, Mistry M, Guaraldi M. [18F]-RP1012: a novel myocardial perfusion imaging agent for use with positron emission tomography (PET). *Circulation* 2005;112:11–761.

[75] Madar I, Ravert HT, Du Y, Hilton J, Volokh L, Dannals RF, et al. Characterization of uptake of the new PET imaging compound 18 F-fluorobenzyl triphenyl phosphonium in dog myocardium. *J Nucl Med* 2006;47:1359–66.

[76] Yu M, Guaraldi MT, Mistry M, Kagan M, McDonald JL, Drew K, et al. BMS-747158-02: a novel PET myocardial perfusion imaging agent. *J Nucl Cardiol* 2007;14:789–98.

[77] Maddahi J, Czernin J, Lazewatsky J, Huang SC, Dahlbom M, Schelbert H, et al. Phase I, first-in-human study of BMS747158, a novel 18F-labeled tracer for myocardial perfusion PET: dosimetry, biodistribution, safety, and imaging characteristics after a single injection at rest. *J Nucl Med* 2011;52:1490–8.

[78] Pysz MA, Gambhir SS, Willmann JK. Molecular imaging: current status and emerging strategies. *Clin Radiol* 2010;65:500–16.

[79] Agdeppa ED, Spilker ME. A review of imaging agent development. *AAPS J* 2009;11:286–99.

[80] Centers for Medicare & Medicaid Services, Office of the Actuary. National Health Expenditure Projections 2011–2021: http://www.cms.gov/Research-Statistics-Data-and-Systems/Statistics-Trends-and-Reports/NationalHealthExpendData/Downloads/Proj2011PDF.pdf, 2012.

[81] O′Donnell M, Wei CW, Xia J, Pelivanov I, Jia C, Huang SW, et al. Can Molecular Imaging Enable Personalized Diagnostics? An Example Using Magnetomotive Photoacoustic Imaging. *Ann Biomed Eng* 2013;41: 2237–47.